JOURNAL OF MATERIALS SCIENCE 21 (1986) 768–774

Effects of attrition milling and post-sintering heat treatment on fabrication, microstructure and properties of transformation toughened ZrO_2

F. F. LANGE
Rockwell International Science Center, Ceramics Group, Thousand Oaks, California 91360, USA

H. SHUBERT, N. CLAUSSEN, M. RUHLE
Max Planck Institut für Mettalforschung, Institut für Werkstoffwissenschaften, Stuttgart, FRG

The effect of attrition milling and post-sintering heat treatment on the fabrication, phase relations, microstructure and properties of ZrO_2 (+2.3 vol% Y_2O_3) powder used to produce a transformation toughened material was examined. Powder used to fabricate the unmilled material was treated and consolidated by a colloidal method. The same powder, treated and consolidated by the same method, but ball milled in a commercial alumina mill before consolidation, was used to fabricate the milled material. Both materials were sintered at 1400° C for 1 h and then heat treated at higher temperatures. Milling introduced Al_2O_3 inclusions (<1 vol%) and a glass phase (7 to 10 vol%). The milled powder was more difficult to sinter and exhibited more bloating (density decrease) during subsequent heat treatment. Transmission electron microscopy observations indicated that the larger glass content of the milled material beneficially reduced residual stresses that arose due to thermal contraction anistropy. Post-sintering heat treatment at temperatures >1450° C produced detectable amounts of cubic ZrO_2 consistent with previously reported phase studies of the ZrO_2–Y_2O_3 system. The development of a bimodal grain structure was concurrent with the formation of detectable cubic phase. The larger grains in this bimodal distribution were primarily observed on the external surface and co-ordinating pores produced during the post-sintering heat treatments which were responsible for the bloating phenomenon. It is hypothesized that the pores were produced by the release of high pressure oxygen during cubic phase formation. Both fracture toughness (K_c) and hardness of the as-sintered materials were unaffected by milling. Hardness decreased with bloating and the decrease was more pronounced for the milled material which exhibited more bloating.

1. Introduction

Attrition milling, for example ball milling, vibromilling, etc. is a customary step practised in both the research laboratory and the factory to prepare ceramic powders for subsequent steps in fabricating dense shapes by sintering. This practice, originally devised by manufacturers of traditional ceramics (e.g. whitewares, refractories, etc.), was the last stage of particle size reduction and was also used to mix the mined, raw materials in preparation for forming the desired powdered shapes that could be sintered at a reasonable temperature. For traditional ceramics, impurities introduced during attrition milling were usually insignificant relative to impurities already present in the raw materials. Today, advanced ceramics are being developed for applications ranging from electronic packaging to advanced heat engines. Powders used for these new ceramics are commonly produced from purified reactants (e.g. gases, liquids, hydroxides, alkoxides, etc.). Although the crystallite size of these purer powders can be $< 1\ \mu m$, attrition milling is still used to break apart hard agglomerates formed by partial sintering of the crystallites at the reaction temperature, and also for mixing of second phases. The reduction of agglomerate size is necessary not only to increase sinterability, but also to eliminate (or reduce) the crack-like voids produced by the differential shrinkage of agglomerates relative to the surrounding powder. For these new powders, impurities introduced during attrition milling can be significant relative to the unmilled powder.

Alternative powder treatments, based on the sedimentation of dilute powder–liquid, colloidal suspensions, can be used to eliminate agglomerates larger than a chosen size [1]. Experience suggests that this method results in a greater probability that agglomerates will be eliminated relative to milling. One might also suspect that this colloidal treatment would also result in fewer impurities. To test this hypothesis and to determine the influence of impurities introduced by milling on fabrication and properties, a study was initiated to compare materials fabricated by the col-

0022–2461/86 $03.00 + .12

loidal sedimentation method to the conventional method of attrition milling.

Zirconia powder containing 2.3 mol % Y_2O_3 was chosen for this study, since it can produce a strong, transformation toughened material. Commercial Al_2O_3 based ball mills and milling media* were used because of their common use throughout the ceramic industry and in research laboratories. The Al_2O_3 used to fabricate these mills contains a silicous glass†. Studies of materials produced by the two powder treatment methods included effects of contaminants on phase relations, microstructural changes, fracture toughness and high resolution microscopy.

2. Experimental details

The as-received ZrO_2 powder used for this study contained large, hard agglomerates produced during the conversion of $ZrOCl_2$ plus a soluble yttrium salt to a $Zr_{(1-x)}Y_xO_{2-x/2}$ ($x = 0.045$ or 2.3 mol % Y_2O_3) powder at elevated temperatures. The powder also contained large, soft agglomerates. A colloidal treatment was used to break apart the soft agglomerates and to eliminate large, hard agglomerates. This treatment was used to prepare powder for both the unmilled and milled materials.

The colloidal treatment [1] involved dispersing the as-received powder in sufficient water to obtain 3 vol % solids at pH = 2 with HCl, sedimenting the dispersion three times to eliminate all particles and hard agglomerates $> 1\,\mu m$, and then spontaneously flocculating the suspension containing particles and hard agglomerates $< 1\,\mu m$ by changing the pH to 7 with additions of NH_3OH. Flocculating concentrates the solids and prevents further mass segregation due to sedimentation during storage. Excessive salts due to HCl and NH_3OH additions were minimized by repeated washing of the flocculated materials. Washing was performed after flucculating by removing the clear supernate, adding distilled water, mixing and reflocculating without acid or base additions. Table I lists the Y_2O_3 content and impurities observed in this powder after the above treatment.

A portion of the flocculated slurry was redispersed by adding HCl to lower the pH to 2. This portion was ball milled in a Al_2O_3 mill for 16 h, poured into a plastic container, and immediately reflocculated by changing the pH to 7 with NH_3OH.

Cylindrical specimens of both the unmilled and milled flocculated slurries were consolidated by filtration (slip casting on plaster). After drying, the specimens were isopressed at 350 MPa and then sintered at 1400° C for 1 h. After sintering, all specimens were diamond ground and polished. Different specimens of each material (namely, unmilled and milled) were heat treated for 1 h at temperatures ranging from 1350 to 1650° C. Densities were determined by the Archimedes method, phases were determined by X-ray diffraction analysis (XRD), the polished and heat treated surfaces were observed with the scanning electron microscope (SEM), the hardness (H) and critical stress intensity factor (K_c) were determined as a function of heat treatment using an indentation technique [2] (20 kg load), and both as-sintered materials were ion thinned for high resolution transmission electron microscopy (TEM) observations. After observations were made on the heat treated surfaces, the interior was examined with the SEM after diamond grinding, polishing and thermal etching at 1350° C for 1 h.

TABLE I Cation content* of unmilled ZrO_2 powder

Ca	4000
Hf	2.1%
P	1180
Si	760
Ti	1000
Y_2O_3	4.10% (2.28 mol %)

*Analysis in p.p.m. unless noted: cations < 500 p.p.m. not shown. Courtesy of Teledyne Wah Chang Albany.

3. Results

3.1. Density

Previous studies have shown that the ZrO_2 (+2.3 mol % Y_2O_3) powder treated and consolidated in the manner outlined above could be sintered at 1400° C for 1 h to achieve a density ≥ 98% of theoretical ($\varrho_t = 6.07\,g\,cm^{-3}$) without the isopressing step [1]. Preliminary work for this study showed that porous materials with densities $< 5.50\,g\,cm^{-3}$ were obtained when the powders were milled before consolidation. Isopressing, prior to sintering, was used to help remedy this situation. Isopressing increases the bulk density of the dried powder compact from 33 to 48% of the theoretical density. This observation suggests that the milled powders were less sinterable than the unmilled powders.

Densities are reported in Table II as a function of heat treatment temperature. A density of > 98% of theoretical ($\varrho_t = 6.07\,g\,cm^{-3}$) could be obtained for the unmilled powder sintered at 1400° C for 1 h, whereas the milled powder resulted in a significantly lower density. SEM observations of sectioned and polished surfaces of milled material sintered at 1400° C for 1 h did not reveal porosity. As reported in the subsequent section, the milled material contained a small amount of Al_2O_3 (< 1 vol %) and a significant amount of a glass. Based on the observation of the insignificant porosity and the significant glass content, it was concluded that the glass was the principal cause for the lower density. Assuming that the density of the glass lies between 2.2 and $3.5\,g\,cm^3$, the volume fraction of the glass in the milled material was calculated‡ to lie between 0.07 and 0.10, respectively.

As reported in Table II, the density of both materials increased slightly when heat treated at 1450° C for 1 h. Heat treatments at higher temperatures resulted in a

*Norton Co., Akron, Ohio, USA. 85% Al_2O_3, 11% SiO_2, 1.2% CaO, 2.0% MgO.

†Purer Al_2O_3 mills and media are large grain materials and wear at an unacceptable rate.

‡Volume fraction of glass $= \dfrac{(\varrho_{specimen} - \varrho_{ZrO_2})}{\varrho_{glass} - \varrho_{ZrO_2}}$.

TABLE IIa Unmilled ZrO_2 (2.3 mol % Y_2O_3) material

Heat treatment temperature (° C)	Density ($g\,cm^{-3}$)	Phases	Grain size† (μm)	H (GPa)	K_c ($MPa\,m^{1/2}$)
1350	5.99	t	0.30	11.7	5.80
(1400)*	5.99	t	–	–	–
1450	6.07	t	0.31	12.1	5.80
1500	5.99	t + c	0.52	12.0	5.85
1550	5.97	t + c	0.58	11.7	5.88
1600	5.93	t + c	0.68	11.6	6.25
1650	5.85	t + c	–	11.2 (10.0)‡	6.48 (6.68)‡

*No heat treatment.
†Smaller grains in bimodal distribution only.
‡Section surface measurements.

TABLE IIb Milled ZrO_2 (2.3 mol % Y_2O_3) material

Heat treatment temperature (° C)	Density ($g\,cm^{-3}$)	Phases	Grain size† (μm)	H (GPa)	K_c‡ ($MPa\,m^{1/2}$)
1350	5.76	t	0.29	11.8	6.00
(1400)*	5.76	t	–	–	–
1450	5.81	t + c	0.34	11.1	5.86
1500	5.66	t + c	0.44	10.3	6.07
1550	5.54	t + c	0.72	9.5	6.06
1600	5.37	t + c	–	8.7	5.95
1650	5.25	t + c	–	7.8	6.28

*No heat treatment.
†Smaller grains in bimodal distribution only.
‡Section surface measurements.

decrease in density, which was more pronounced for the milled materials. Since all heat treated specimens were pre-sintered at 1400° C for 1 h, the loss of density at heat treatment temperatures > 1450° C must be caused by a bloating phenomenon, i.e. the release of a high pressure gas. Observations of sectioned and polished specimens showed the development of large, spherical pores which increased in size with heat treatment temperature. For the same heat treatment temperature, the pores were larger for the milled material. Fig. 1 illustrates these pores for the milled material heat treated at 1650° C for 1 h. Pores were not observed on the polished and heat treated surfaces; sectioning showed that a 20 to 30 μm surface layer was pore-free.

3.2. Phase content

Only the t phase could be detected in the as-sintered materials. Small amounts of the cubic phase would be difficult to detect by XRD since the diffraction peaks are nearly coincident with the tetragonal phase in this system. The compositional boundaries of the t + c two-phase field has been defined by three contradictory phase studies. For the temperatures of interest here (1300 to 1600° C), Srivastava *et al.* [3] indicated that the two-phase field extends from 3.0 to 7.5 mol % Y_2O_3 with the t → m + c eutectoid composition and temperature of 3.5 mol % Y_2O_3 and 565° C (Scott [4] and Stubican *et al.* [5] appear to agree). Pascual and Duran [6] suggest similar bounds on the two-phase field within this temperature range, but indicate that the eutectoid is at 4.5 mol % Y_2O_3 and 490° C. Ruh *et al.* [7], on the other hand, indicate that "...a two-phase solid solution plus cubic solid solution exists from 1.5 to 7.5 [mol]% Y_2O_3 from 500° C to 1600° C". The results of Ruh *et al.* [7] would place our as-sintered composition (2.3 mol % Y_2O_3) within the two-phase field (containing ~ 10 vol % cubic phase), whereas the other studies would place our material in the single-phase, tetragonal field. The monoclinic (m) phase was never observed by XRD in the as-sintered or heat treated materials unless their surfaces were diamond ground. It is well known that surface grinding can stress-induce the t → m transformation [8].

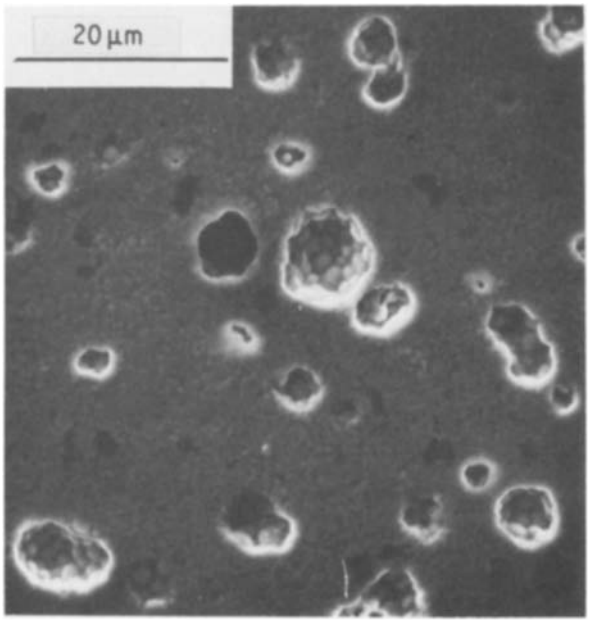

Figure 1 Bloating voids produced in the milled material heat treated at 1650° C for 1 h. Dark areas are Al_2O_3 contaminated grains.

As reported in Table II, the cubic (c) phase was observed in the heat treated materials. The cubic phase was first observed at 1450° C for the milled material and at 1500° C for the unmilled material. For both materials, the fraction of cubic phase increased with heat treatment temperature. The occurrence of the cubic phase is consistent with previous phase equilibria studies [3–7] which shows that the tetragonal phase initially fabricated at lower temperatures will decompose into two new compositions with tetragonal (t′) and cubic (c) structures, respectively.

SEM examination of the milled materials also revealed large Al_2O_3 particles, one of the contaminants introduced during milling, as shown in Fig. 2. The Al_2O_3 particles are easily observed with SEM due to much lower atomic number of aluminium relative to zirconium.

High resolution TEM showed that both unmilled and milled materials contained a silicous glass phase, as shown in light and dark-field micrographs in Fig. 3. The dark-field micrographs were obtained by imaging the electrons scattered by the glass which enhances the contrast between the glass and crystalline phases. Milled material contained large pockets of glass, typical of Fig. 3b, whereas the much smaller pockets in the unmilled material were confined to three or four grain junctions, typical of Fig. 3a. Glass was also present at all the grain boundaries observed in the

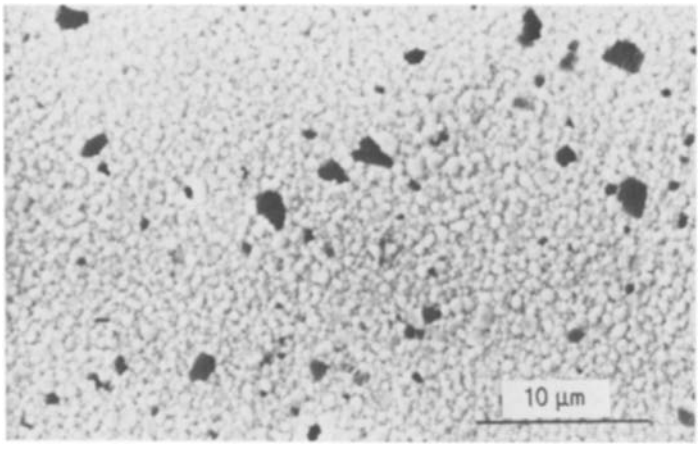

Figure 2 Distribution of Al_2O_3 grains introduced during milling.

milled material and most (if not all) boundaries in the unmilled material. Note the rounded grains in the milled material (Fig. 3b) indicative of a large liquid content at the sintering temperature, relative to the straighter boundaries in the unmilled material.

Energy dispersion X-ray analysis (EDAX) showed silicon, aluminium and yttrium present in the glass, indicating that some of the yttrium diffused from the ZrO_2 into the liquid silicate during fabrication. The ZrO_2 in the milled material was also observed to contain a detectable amount of aluminium, indicative of some reaction between the ZrO_2 and Al_2O_3 or glass during sintering.

The most interesting TEM observation concerned differences in the strain fields between the two materials. The unmilled material was highly strained, making imaging much more difficult due to strain contrast. Much of the thin foil of the unmilled material disintegrated due to the t → m transformation during ion milling. Grain boundary cracks were frequently observed between untransformed t grains (see arrow in Fig. 3a). By contrast the grains in the milled material contained smaller strains and were easier to image. This observation strongly suggests that the larger amount of glass (viscous liquid at higher temperatures) in the milled material relieves much of the residual stresses developed during cooling due to the anisotropic thermal contraction of the tetragonal ZrO_2 grains.

3.3. Grain growth

The grains in both materials sintered at 1400° C for 1 h, sectioned, polished and thermally etched at 1350° C were nearly identical in average size (0.3 μm) and had a relatively narrow size distribution. A bimodal distribution developed at higher heat treatment temperatures. The development of the bimodal distribution (first observed at 1450° C for milled material and 1500° C for unmilled material) was much more pronounced for the milled material. Fig. 4b illustrates the subtle development for the unmilled material between 1450 and 1550° C, and in Fig. 4a, the more pronounced development for the milled material over the same temperature range is shown. At the highest treatment temperature (1650° C for 1 h), the large grains ($\sim 10\ \mu$m) completely covered the surface of the milled material. For the same temperature, the bimodal distribution and average size of the largest grains ($\sim 5\ \mu$m) remained the same, as shown in Fig. 4b, at 1550° C. Table I reports the average size of the smaller grains within the bimodal distribution as measured by the line intercept method without correction for either grain volume or shape.

Although the heat treated surfaces of the two materials were very different, grain size and distribution of sectioned surfaces thermally etched at 1350° C for 1 h were indistinguishable, and were identical to that of the unmilled materials, as shown in Fig. 4b. The pores developed at higher heat treatment temperatures were co-ordinated by larger grains, as shown in Fig. 1.

Smaller grains were frequently included in the larger grains, as shown in Fig. 5. The smaller grains are also located at three (or four) grain junctions, suggesting that they impede the growth of the larger cubic grains as observed for other two-phase material [9]. Previous transmission electron microscope observations [10, 11] have shown that the larger grains in similar materials are cubic and the smaller grains are tetragonal.

Indentation K_c mesasurements[§] were made on the outer surfaces of the thermally treated unmilled material and on the sectioned surfaces of the milled material. Average values, reported in Table II, indicate that the fracture toughness of the two as-sintered materials are nearly identical (5.8 and 6.0 MPa $m^{1/2}$). K_c changed little ($< 10\%$) with heat treatment temperature.

Table II also reports that the hardness (H), measured on the dense surface (unmilled material), only decreases by $\sim 8\%$ with increasing temperature, despite the increased porosity of the underlying bulk material. The large decrease in hardness ($\sim 35\%$) for measurements of the sectioned, milled material more strongly reflects the increasing porosity with heat treatment temperature.

4. Discussion

As expected, milling unavoidably introduced contaminants, namely large Al_2O_3 inclusions, and a large frac-

[§]This technique requires knowledge of the material's elastic modulus, which was assumed to be 207 GPa for all materials regardless of density.

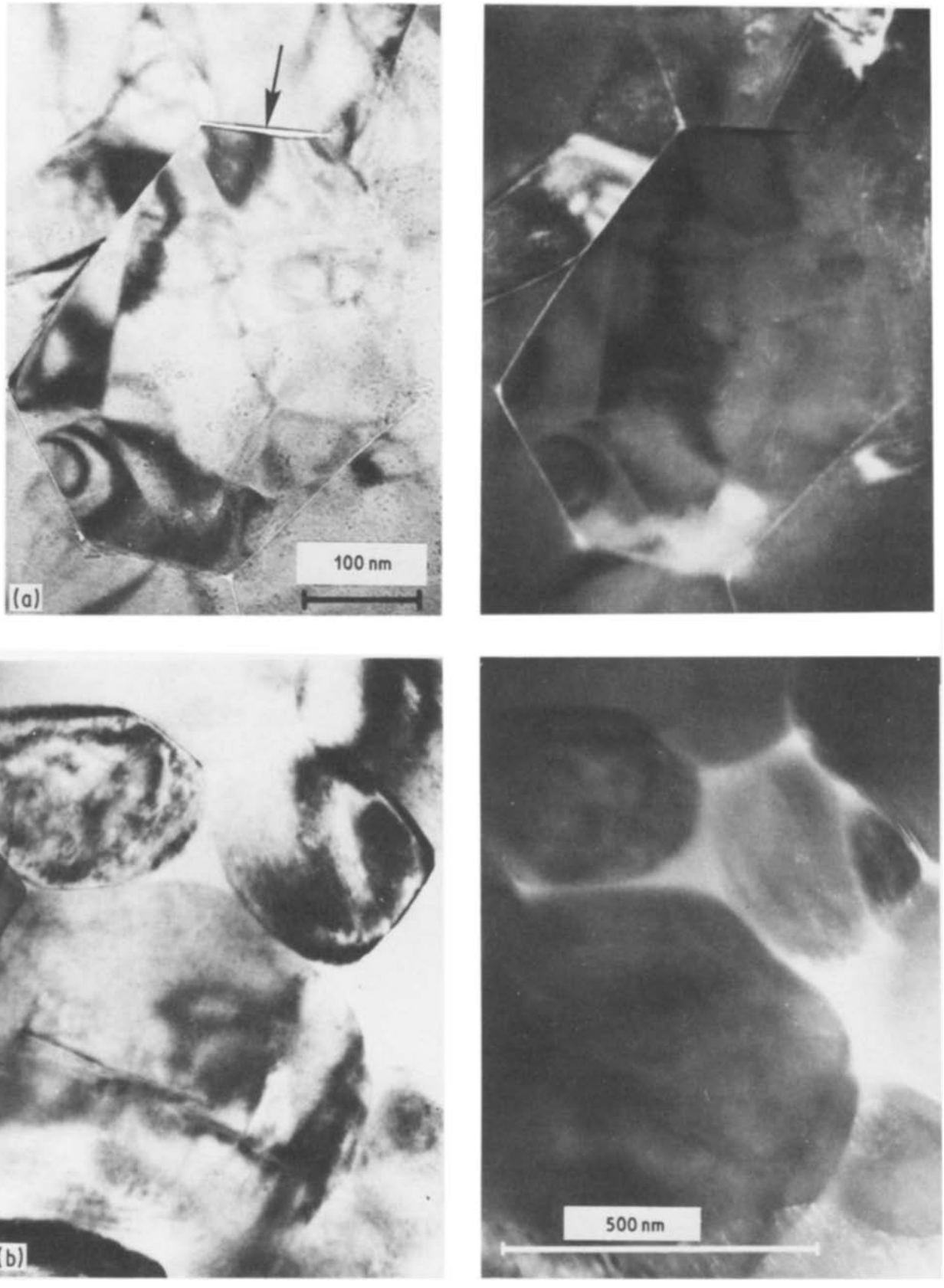

Figure 3 (a) Unmilled, sintered ZrO_2 (+2.3 mol % Y_2O_3) material (arrow points to crack); (b) milled, sintered ZrO_2 (+2.3 mol % Y_2O_3). Both (a) and (b) show light- and dark-field images to show the presence of glass.

tion of glass. For the ZrO_2 (+2.3 mol % Y_2O_3) studied, the contaminants altered sinterability, bloating behaviour, phase relations, grain growth and residual stresses. Although not studied, the large Al_2O_3 inclusions can also be considered as an unwanted flaw population.

The decrease in sinterability of the milled material was surprising, i.e. one would expect the larger volume fraction of silicate liquid to increase the sinterability of ZrO_2. The authors have no consistent explanation for this observation.

As reported, the cubic structure was first detected in

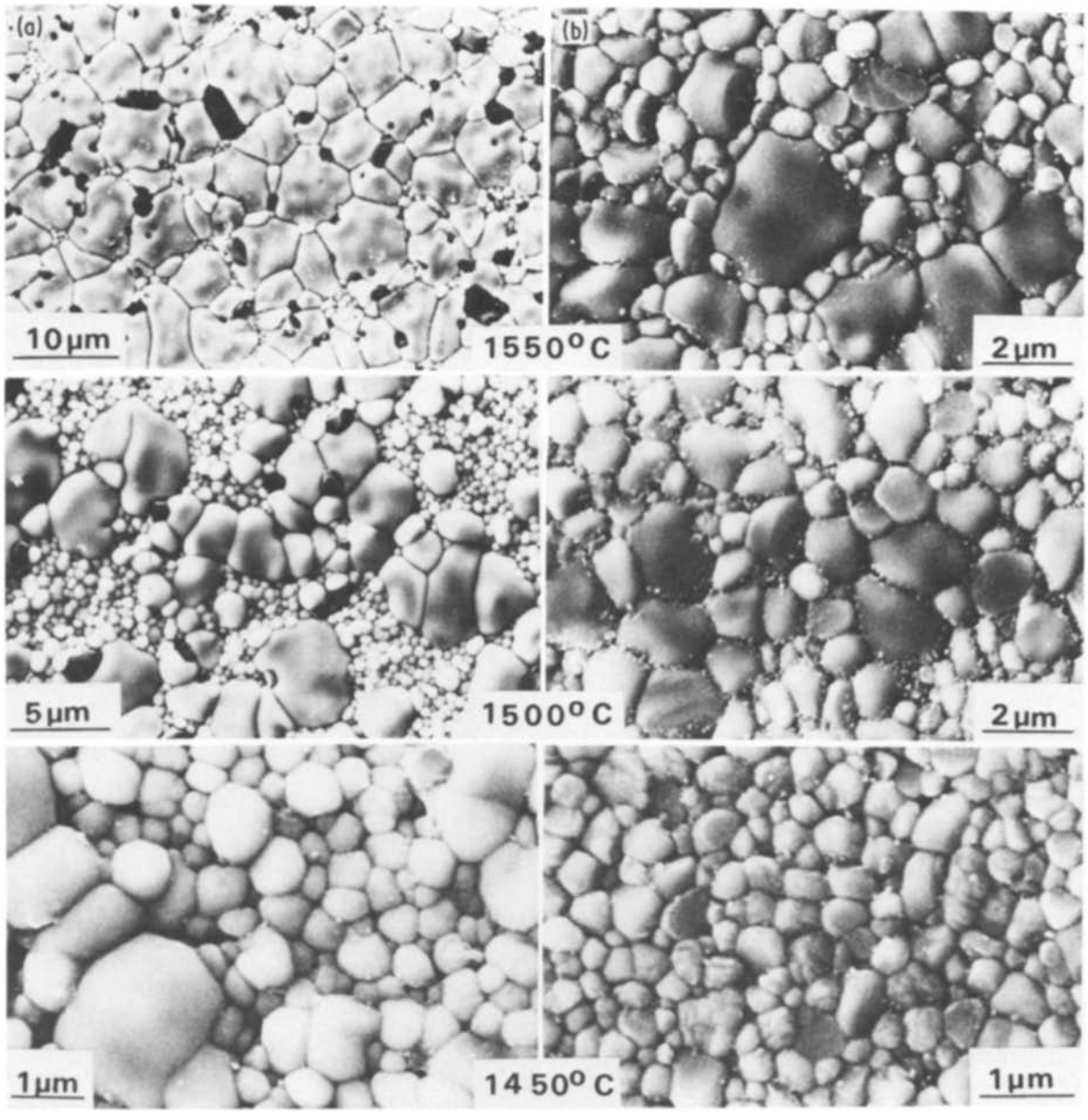

Figure 4 Grain structures of polished and heat treated materials. (a) Milled material (dark grains are Al_2O_3); (b) unmilled material.

the milled material at a temperature 50° C lower than for the unmilled material. Limited aluminium solid solublity was observed in the milled (Al_2O_3 contaminated) material and is reported elsewhere [10]. If the limited solid solubility of Al^{3+} has a similar effect as Y^{3+} in the ZrO_2 structures, the milled material would contain a greater equivalent amount of Y_2O_3 (i.e. $Y^{3+} + Al^{3+}$). The net effect of both Y^{3+} and Al^{3+} would cause the milled material to contain more cubic phase relative to the aluminium-free, unmilled material.

Grain growth in both materials was initiated by the occurrence of abnormally large grains which were predominately found either on the external surface or co-ordinating voids that grew during heat treatment to produce bloating. The observation of the larger grains coincided with observation of the cubic phase, strongly suggesting that the larger grains are the cubic phase, as indicated by others for similar materials [11, 12]. Previous phase equilibria work [3–7] has shown that the volume content of the cubic phase should increase with increasing heat treatment temperature for the composition studied here, namely the tetragonal phase produced at lower (sintering) temperatures will partition into a new tetragonal phase and a cubic phase. The partitioning reactions require the interdiffusion of all ionic species (namely zirconium, yttrium and oxygen). That is, the new tetragonal phase becomes enriched with zirconium and oxygen and depleted of yttrium whereas regions forming the new cubic phase become enriched with yttrium while rejecting zirconium and oxygen. Since the cubic phase did not form as precipitates within the tetragonal grains which requires relatively short range diffusion, but developed as abnormally large grains at external and internal surfacces, one might conclude that the cubic grains at these surfaces grew under non-equilibrium conditions.

The bloating phenomenon, which must be caused by a reaction that produces high pressure gas, was accentuated in the milled material containing more of the viscous silicate phase which would allow a greater

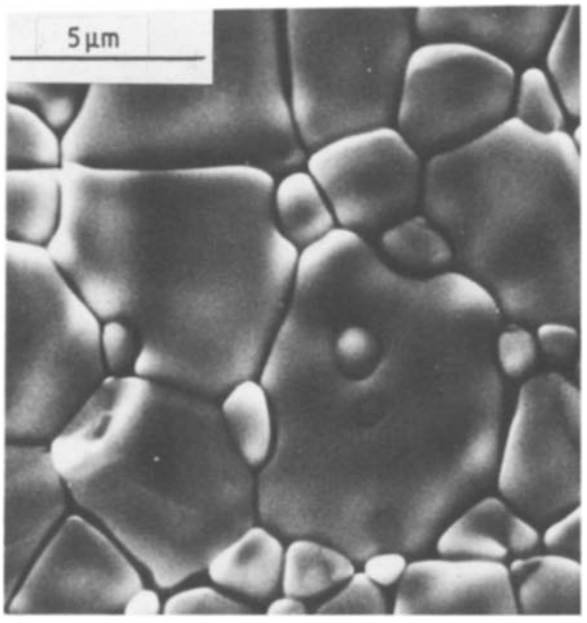

Figure 5 Grain structure of unmilled material (heat treated at 1650° C for 1 h) showing included smaller grain.

deformation. It is hypothesized that the partitioning reaction (production of cubic phase) is responsible for the bloating and that the release of high pressure oxygen was responsible for the bloating phenomenon. This hypothesis is based on (a) the fact that the larger (cubic) grains co-ordinate the spherical voids responsible for the bloating phenomenon, and (b) previous phase equilibria studies [3–7] that show that cubic phase formation during the partitioning reaction is accompanied by the rejection of oxygen. It should be pointed out that release of oxygen into the environment requires charge compensation within the zirconia structure. Zirconia is known to lose oxygen in low partial pressures of oxygen [13, 14] at high temperatures producing "...vacancy aggregates which ultimately produced colloidal metallic particles".

Residual stresses that arise during cooling by thermal contraction anistropy can produce microcracking, either during cooling itself or upon subsequent tensile stressing. The magnitude of these residual stresses not only depends on the coefficient of differential thermal contraction, but also on stress relaxation phenomena. It is quite obvious that the large glass content in the milled material beneficially relaxes residual stresses during cooling. This observation has many implications with regard to engineering with stronger and more wear-resistant ceramics for lower temperature use.

Acknowledgement

The technical work of B. Davis is certainly appreciated. A portion of this work was performed while F. Lange at the Powder Metallurgy Laboratory at the Max Planck Institut für Metallforschung in Stuttgart. Work was performed under AFOSR Contract No. F49620-81-C-0036.

References

1. F. F. LANGE and B. I. DAVIS, *Amer. Ceram. Soc.* in press.
2. A. G. EVANS and E. A. CHARLES, *J. Amer. Ceram. Soc.* **59** (1976) 371.
3. K. K. SRIVASTAVA, R. N. PATIL, C. B. CHAUDHARY, K. V. GOKHALE and E. C. SUBBARAO *Trans. J. Brit. Ceram. Soc.* **73** (1975) 85.
4. H. G. SCOTT *J. Mater. Sci.* **10** (1975) 1527.
5. V. S. STUBICAN, R. C. HINK and S. P. RAY, *J. Amer. Ceram. Soc.* **61** (1978) 17.
6. C. PASCUAL and P. DURAN, *ibid.* **66** (1983) 23.
7. R. RUH, K. S. MAZDIYASNI, P. G. VALENTINE and H. O. BIELSTEIN, *ibid.* **67** (1984) C-190.
8. D. J. GREEN, F. F. LANGE and M. R. JAMES, *ibid.* **66** (1983) 623.
9. F. F. LANGE and M. M. HIRLINGER, *ibid.* **67** (1984) 167.
10. M. J. BANNISTER, *J. Aust. Ceram. Soc.* **18**(1) (1982) 6.
11. K. TSUKUMA, Y. KUBOTA and T. TSUKIDATA, in "Advances in Ceramics", Vol. 12; edited by Nils Claussen, Manfred Ruhle and Arthur H. Heuer (American Ceramic Society, Columbus, 1984).
12. M. RUHLE, N. CLAUSSEN and A. H. HEUER, *ibid.* p. 352.
13. R. RUH and H. J. GARRETT, *J. Amer. Ceram. Soc.* **50** (1967) 258.
14. D. A. WRIGHT, S. S. THORP, A. AYPAR and H. P. BUCKLEY, *J. Mater. Sci.* **8** (1973) 876.

Received 21 March
and accepted 2 April 1985